Journal of the Australian Ceramic Society
https://doi.org/10.1007/s41779-026-01352-x

RESEARCH

Use of İzmit Gulf bottom sludge as a raw material component: eco-friendly wall tile glaze composition

Nermin Demirkol[1] · Kübranur Çatalbaş[2] · Neslihan Tamsü Selli[2]

Received: 19 August 2025 / Revised: 7 January 2026 / Accepted: 20 January 2026
© The Author(s) 2026

Abstract

This study investigates the reuse of İzmit Gulf bottom sludge as a silica substitute in black opaque wall tile glazes. The sludge, containing 44.64 wt% SiO_2 and 7.47 wt% Fe_2O_3, was incorporated at 25–100 wt% replacement rates. Viscosity measurements showed that higher sludge levels significantly increased viscosity from 460 to 920 mPa·s. Thermal analyses revealed that sintering and softening temperatures rose from 734 °C to 798 °C (STD) to 798 °C and 832 °C (S4), demonstrating improved refractory behavior. Microhardness values peaked at ~720 Hv in the S1 composition (25 wt% sludge), exceeding both the reference glaze (~650 Hv) and higher sludge samples, which showed reduced hardness due to porosity. Gloss decreased progressively from 92 (STD) to 75 (S4), while color parameters remained stable. Leaching tests confirmed that all heavy metals stayed within regulatory limits, although chromium release increased to 0.03 mg/L in S4 but remained below the 0.05 mg/L threshold. Therefore, S1 composition offered the most balanced performance, combining improved hardness, acceptable gloss, and environmental compliance. The findings demonstrate that İzmit Gulf sludge can be valorized as a sustainable glaze raw material when used in controlled proportions, supporting resource conservation and waste minimization in ceramic production.

Keywords İzmit Gulf · Bottom sludge · Waste · Glaze · Eco-friendly composition

Introduction

The ceramic tile industry is significantly transforming towards integrating sustainable manufacturing practices, challenges in securing critical raw materials, and increasingly stringent waste management regulations. The gradual depletion of natural resources such as feldspar, clay, kaolin, quartz, etc., and pandemic issues have emphasized the urgency of identifying locally available alternative raw materials. Simultaneously, the global rise in industrial, construction, and demolition waste presents considerable potential for material recovery and reuse. Incorporating such waste streams into ceramic tile production reduces the consumption of virgin resources and the environmental burden associated with their extraction and transportation. It aligns with resource-efficient economy principles by converting waste into valuable inputs. Indeed, recent literature demonstrates that many types of waste, when subjected to appropriate pre-treatment and characterization, can exhibit comparable or even superior structural and functional properties to those of conventional raw materials [1–5]. In this context, integrating secondary raw materials into production systems is an environmental consideration and a strategic imperative for ensuring the ceramic sector's sustainability, raw material security, and technological innovation capacity. In addition to waste generated from industrial processes, recent studies have also focused on the valorization of marine sediments as alternative raw materials for construction materials due to their silicate-rich composition and widespread availability. Some of these sediments have been used in the production of concrete materials [6, 7], bricks [8, 9], cement [10, 11], paving blocks [12, 13], mortar [14, 15], and as road construction material [16–18]. In this context, the dredged marine sediments from the İzmit Bay—one of the most industrialized and densely populated coastal zones in northwestern Turkey—represent a significant

✉ Neslihan Tamsü Selli
ntamsu@gtu.edu.tr

[1] Department of Ceramics, Kocaeli Üniversitesi, Kocaeli, Türkiye

[2] Department of Materials Science and Engineering, Gebze Technical University, Kocaeli, Türkiye

Published online: 29 January 2026

Table 1 Chemical analysis of İzmit Gulf Bottom Mud

Components	Sediment (wt%)
Al_2O_3	15.74
SiO_2	44.64
Na_2O	3.86
CaO	6.56
TiO_2	0.87
MgO	3.07
K_2O	2.33
Fe_2O_3	7.47
C_2O_3	0.03
P_2O_5	0.15
MnO	0.07
L.O.I.	15.21

environmental burden due to the high annual volumes of extraction and their complex geochemical nature. Recent research indicate that thousands of tons of bottom sludge are removed annually as part of dredging activities aimed at maintaining port functionality and navigational safety.

After undergoing appropriate pre-treatment processes such as drying, grinding, and chemical characterization, İzmit Bay sediments reveal a promising potential as a sustainable substitute for silica and coloring oxides (Fe_2O_3, MnO, etc.) in ceramic wall tile glaze formulations. The aim of this study is to valorize İzmit Gulf Bottom wastes by using them as substitutes for silica and coloring oxides in black glossy opaque frit compositions. In this way, their incorporation not only reduces the dependency on natural raw materials but also enhances the ecological performance of tile production by transforming hazardous or inert waste into value-added inputs. This approach aligns with resource-efficient economy strategies and contributes to raw material security, resource conservation, and waste minimization within the ceramic industry, offering a hopeful outlook for the future of sustainable practices in the ceramic tile industry.

Experimental procedure

The chemical composition of the sediment was determined using XRF analysis (Epson 4 X-Ray Spectrometer, Malvern Panalytical), and the findings are presented in Table 1. The study revealed that the waste material contains notably high levels of silica, alumina, iron oxide, calcium oxide, magnesium oxide, sodium oxide, and potassium oxide. As can be seen, the contents of SiO_2 and Fe_2O_3 in the waste are pretty high. This suggests that the waste could be used as a frit raw material component in dark-colored glazes.

The preparation process of dredged sediment waste and the preparation process of the waste is given in Fig. 1.

In the study, the components and their weight percentages of the standard black, glossy, and opaque frit are presented in Table 2. The bottom sludge was used either partially or entirely in place of silica, while keeping the total silica content in the composition constant. Accordingly, different compositions were prepared by substituting silica with bottom sludge at rates of 25wt. % (S1), 50 wt% (S2), 75 wt% (S3), and 100 wt% (S4), as shown in Table 2. Since the amount of iron oxide derived from the waste is relatively high, no additional iron oxide was added to the formulations. Only a small amount of coloring oxide was added to maintain color balance.

The weighed and throughly mixed batches were melted in alumina crucibles in a laboratory type electrically heated furnace (Protherm PLF 160/7) at 1450 °C for 2 h. The were then quenched by pouring into cold water to obtain frits. Subsequently, the frits were dry-milled to a particle size below 63 microns. For glaze preparation, the frit content was weighed to 90% by weight, kaolin to 8.5% by weight, carboxymethyl cellulose (CMC) to 1.0% by weight, and sodium tripolyphosphate (STPP) to 0.5% by weight. The mixture was adjusted to 50% dry matter content, with the remainder being water. The prepared mixtures were ball-milled for 50 min. The suspensions were applied on the green wall tile bodies. The glazed specimens were fired in a laboratory type electrically heated single fast-firing kiln (Nabertherm LS 12/13) at 1050 °C for 30 min. The viscosities of the suspensions prepared to determine whether the waste material causes any change in the viscosities of

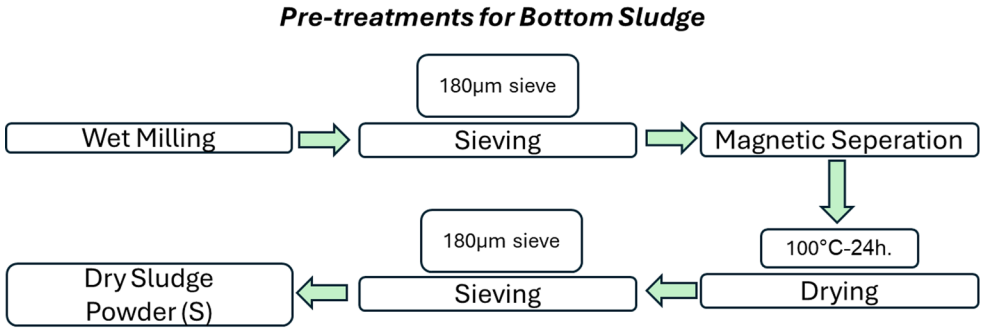


Fig. 1 Pre-treatments of the bottom sludge

Table 2 Standard glossy opaque frit (STD) and other firit compositions with sludge addition

Components	STD	S1	S2	S3	S4
	(wt%)	(wt%)	(wt%)	(wt%)	(wt%)
SiO_2	40.12	37.0	21.20	9.64	-
Sludge	0.00	27.6	47.45	64.67	77.57
B_2O_3	15.05	18.5	15.9	14.46	12.99
Na_2O	10.02	5.42	3.53	2.27	1.24
K_2O	4.02	3.25	1.61	3.35	1.74
CaO	10.02	1.48	3.88	1.16	1.40
ZnO	5.02	5.44	5.26	4.50	4.05
Al_2O_3	5.02	-	-	-	-
TiO_2	3.01	-	-	-	-
Fe_2O_3	5.12	-	-	-	-
Cr_2O_3	0.12	0.05	0.05	0.05	0.05
MnO	2.00	0.86	0.67	0.56	0.45
CoO	0.50	0.50	0.50	0.50	0.50

compositions were also measured. For this purpose, an Anton Paar ViscoQC-100R viscometer was used. The temperature was held constant at 25 °C, with the sample being mechanically pre-mixed at 850 RPM for 1 min. After a 1-minute rest period, the measurement commenced. To assess the settling behavior of the suspensions, viscosity measurements were taken at 1, 5, 10, 30, 60, and 120 min. These values were then compared to those of standard black opaque glaze.

The colouring parameters L*, a* and b* of all samples were measured by Minolta CR-300 series chromometer. Gloss values were measured by a gloss meter (Minolta Glossmeter 268) with 60° light incident angle.

To investigate the melting behavior of the compositions, heat microscopy analyses were carried out by using side-view hot-stage microscope (Misura 3 HSM Hot-stage microscopy, Expert Systems, Srl, Modena, Italy). Each powdered glaze was manually pressed into a pellet (3 mm height × 2 mm dia.) and placed on an alumina substrate. The samples were heated at 10 °C/min to 1050 °C.

XRD analyses were conducted by a Rigaku Rint 2000 series of difractometer with CuKα radiation. XRD patterns were taken from the fired glazed surfaces, working at 40 kV and 30 mA, with 2 °C/min scanning velocity. Glaze microstructures were investigated by SEM fitted with EDX spectrum (Phillips XL30 SFEG).

Microhardness measurements were carried out by hardness testing equipment (Instron Wolpert Tester 2100) with the help of the Vickers indentation method at a load of 50 gf applied for 10 s. At least ten indentations were made for obtaining an average microhardness value for each sample [19].

Since sludge waste was used in the glazed samples, a leaching test was conducted to determine whether potentially hazardous substances such as heavy metals were released from the glaze surface. ICP (Inductively Coupled Plasma) Spectroscopy (PerkinElmer Optima 2100 DV ICP-OES) analyses were subsequently performed for glazed and unglazed samples [20].

Results and discussion

Evaluation of glaze viscosity changes depend on the sludge addition

Whether the bottom sludge waste would cause any change in the viscosity of the glaze compositions was determined through viscosity analyses. Figure 2 illustrates that the viscosity of all glaze suspensions exhibited a time-dependent viscosity increase.

The STD sample demonstrated the lowest initial viscosity, while incorporating bottom sludge, particularly at higher percentages (S3 and S4), resulted in significantly elevated viscosity values throughout the aging period. These findings suggest that bottom sludge promotes the formation of a more interconnected particle network, reducing the overall fluidity of the suspension. The rheological destabilization observed with increased sludge content is critical for understanding and optimizing the processing parameters of glaze formulations containing recycled materials.

Optical and thermal properties of the samples

Table 3 presents the optical properties of the glaze samples formulated with varying proportions of sludge. The L* values, representing lightness, ranged from 26.19 (STD) to 27.43 (S3), indicating only minor brightness variations among the compositions. The a* and b* chromatic coordinates remained relatively stable, suggesting no substantial change in the overall hue with increasing waste content. However, gloss measurements exhibited a marked decline from 92 in the reference glaze (STD) to 75 in S4, reflecting a progressive reduction in surface reflectance

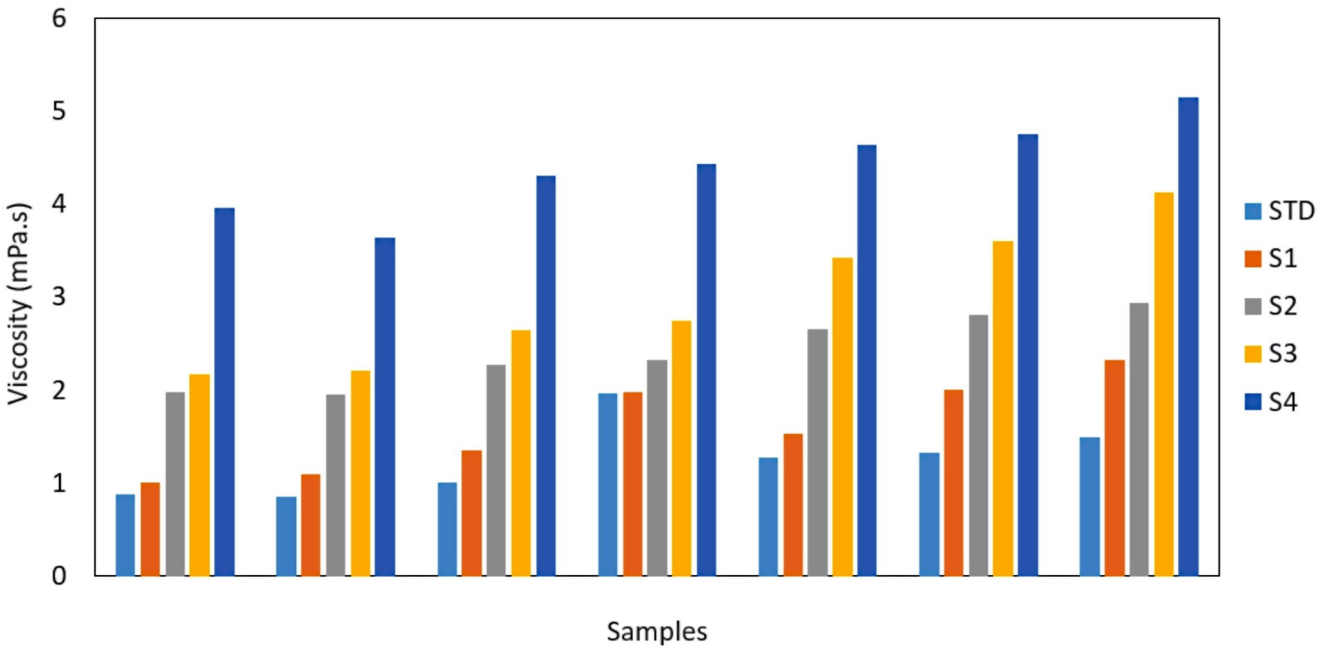


Fig. 2 The graph showing the viscosity values of suspensions varying with time

Table 3 Optical properties of the samples

Samples Code	L*	a*	b*	Glossness (60º)
STD	26.19	0.08	-0.67	92
S1	26.92	0.10	-0.65	90
S2	26.65	0.08	-0.64	87
S3	27.43	0.09	-0.70	83
S4	26.40	0.31	-0.67	75

as the proportion of sludge increased. This trend suggests that while the replacement of sludge material did not significantly impact color coordinates, it had a considerable influence on gloss, potentially due to changes in surface microstructure and homogeneity.

The thermal behavior of the glaze samples was characterized using hot stage microscopy, as illustrated in Fig. 3. Four characteristic temperatures were recorded for each composition: the onset of sintering, softening temperature, hemisphere formation (sphere), and half-sphere deformation stages. For the first sample (STD), sintering began at 734 °C, followed by softening at 798 °C. The sample reached the sphere shape at 970 °C, and further deformation to the half-sphere occurred at 1002 °C. The (S1) sample exhibited a slightly higher onset of sintering (736 °C) and softening (810 °C), with sphere and half-sphere formation at 982 °C and 1026 °C, respectively. The (S2) sample showed a more pronounced increase in thermal resistance, initiating sintering at 765 °C, softening at 826 °C, and forming the sphere and half-sphere shapes at 992 °C and 1030 °C. The (S3) sample presented higher thermal stability, beginning sintering at 798 °C, softening at 830 °C, sphere formation at 1014 °C, and half-sphere formation at 1056 °C. Finally, the (S4) sample demonstrated the highest thermal resistance among all compositions, with sintering onset and softening temperatures of 798 °C and 832 °C, respectively. Sphere and half-sphere deformation were observed at 1024 °C and 1068 °C.

The progressive increase in all characteristic temperatures observed in the hot stage microscopy analysis can primarily be attributed to the combined compositional changes introduced by the gradual replacement of conventional SiO_2 with sludge-derived materials. While the total silica content remained comparable, the sludge contributed significant amounts of Al_2O_3 and Fe_2O_3, both of which are known to enhance the refractory character [21, 22] and viscosity of glassy phases [23–25]. Additionally, the pronounced decrease in alkali oxides (Na_2O and K_2O), which normally act as fluxing agents to lower the melting and softening points [26, 27], further increased the thermal stability of the glazes. The resulting formulations exhibited higher softening, sphere formation, and half-sphere deformation temperatures due to this cumulative effect, indicating that the substitution with sludge not only maintained but reinforced the structural integrity of the glaze network during heating.

Analysis of heavy metal leaching from glazes

To evaluate the environmental safety of the developed glazes, the leaching behavior of selected heavy metals was investigated using inductively coupled plasma (ICP) analysis. Figure 4 presents the ICP analysis results comparing the concentrations of selected critical elements (As, Ba, Cd, Cr,

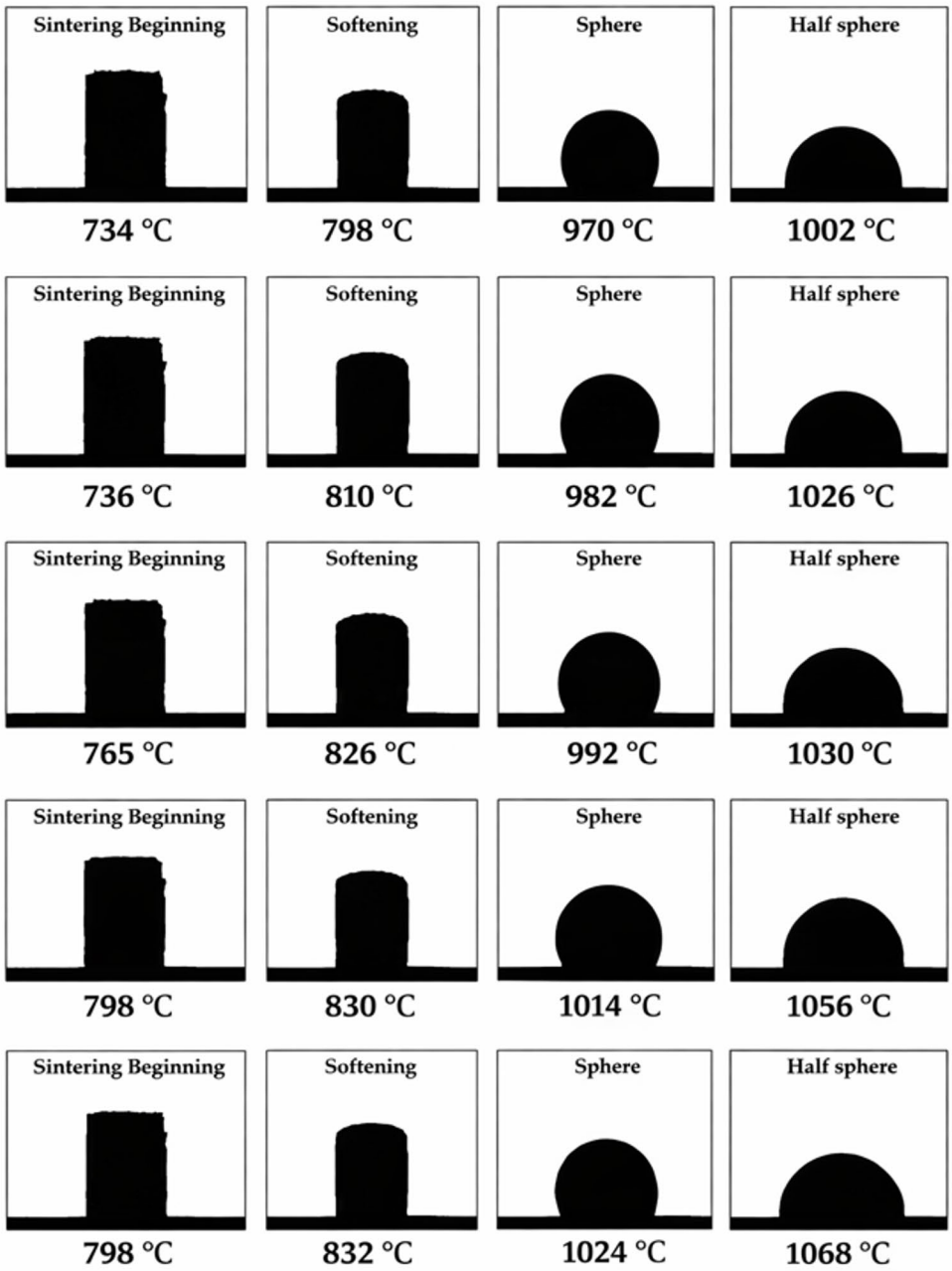


Fig. 3 Results of the hot stage microscopy analysis of the samples

Ni, and Pb) released from the glaze formulations containing increasing proportions of waste-derived sludge. The limit values of the elements were taken from the study by Sisti et al. [20].

Overall, all samples exhibited arsenic, barium, and cadmium concentrations well below the regulatory limit values, indicating that the incorporation of sludge did not significantly contribute to the leaching of these elements. In contrast, chromium concentrations showed a noticeable increasing trend with higher sludge content, reaching approximately 0.03 mg/L in the S4 sample, which remains below the threshold limit of 0.05 mg/L but highlights a potential need for monitoring. It should also be noted that chromium oxide (Cr_2O_3) was intentionally incorporated into the glaze formulations as a colorant pigment to impart specific coloration effects. Therefore, the presence of chromium in the leachates is partly attributable to its role as a functional additive rather than an unintended contaminant. Although the nominal Cr_2O_3 content remained constant or even slightly decreased across the formulations, the observed increase in chromium release in higher sludge-containing samples is likely due to a combination of factors. In particular, the reduction in alkali oxides may have decreased the melt fluidity and hindered the complete encapsulation of chromium

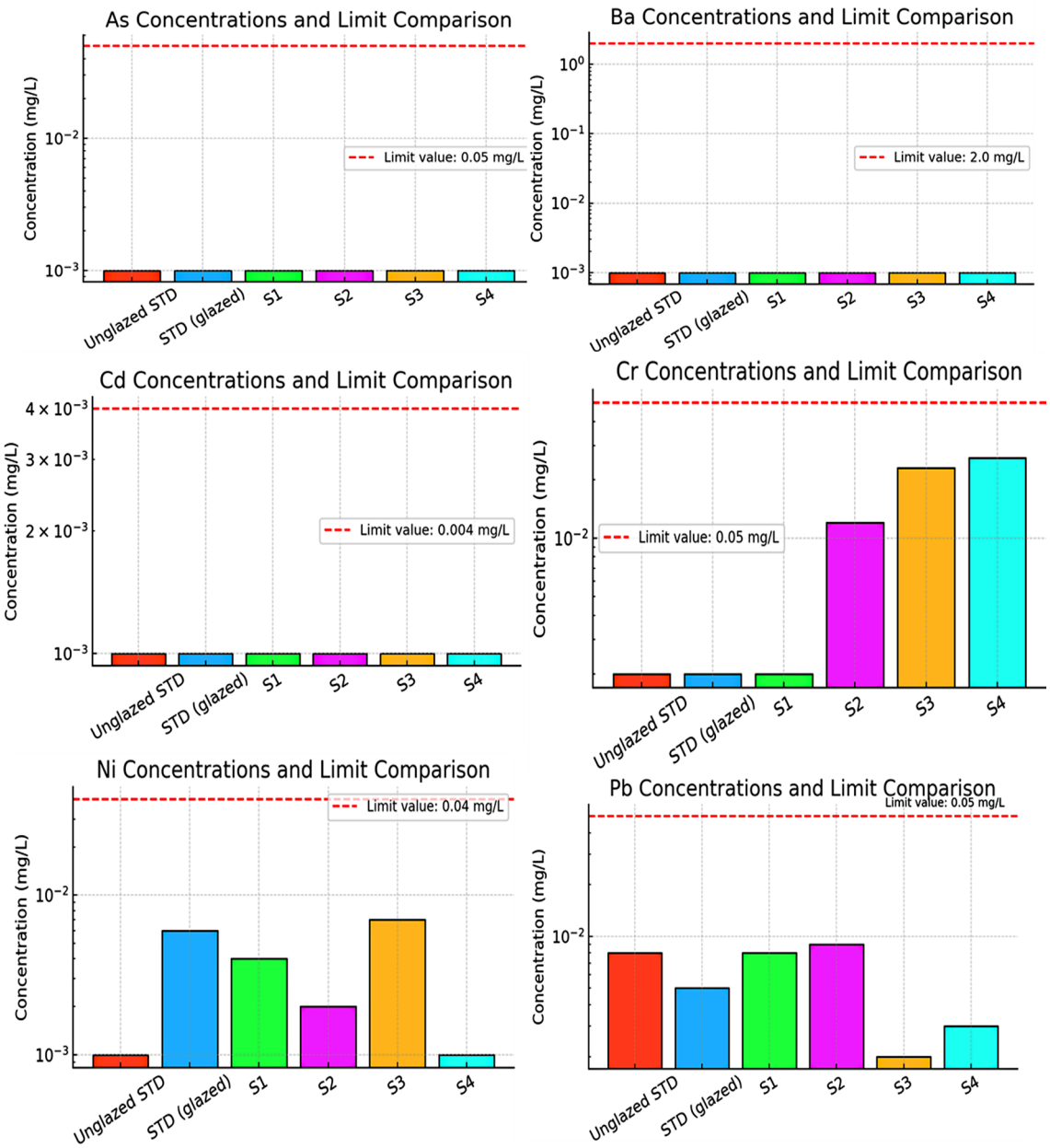


Fig. 4 Graphs of the ICP analysis results for certain critical elements

within the glassy matrix [28, 29]. Furthermore, the elevated content of iron oxide and other transition metals present in the sludge could have altered the redox equilibrium during firing, facilitating partial solubilization of chromium species [30, 31]. This interplay between pigment incorporation and compositional adjustments highlights the importance of carefully controlling both the raw material composition and processing parameters to minimize leaching of potentially hazardous elements. Nickel levels were relatively stable across most formulations and did not exceed the permissible limit. Interestingly, lead concentrations slightly decreased with higher sludge incorporation, suggesting enhanced immobilization within the glaze matrix.

These findings demonstrate that while the majority of heavy metals remained at safe levels, chromium leaching was more sensitive to the sludge content and should be carefully controlled in future formulations.

Phases and microstructural properties of the samples

Figure 5 illustrates the X-ray diffraction (XRD) patterns of the reference glaze (STD) and the formulations containing

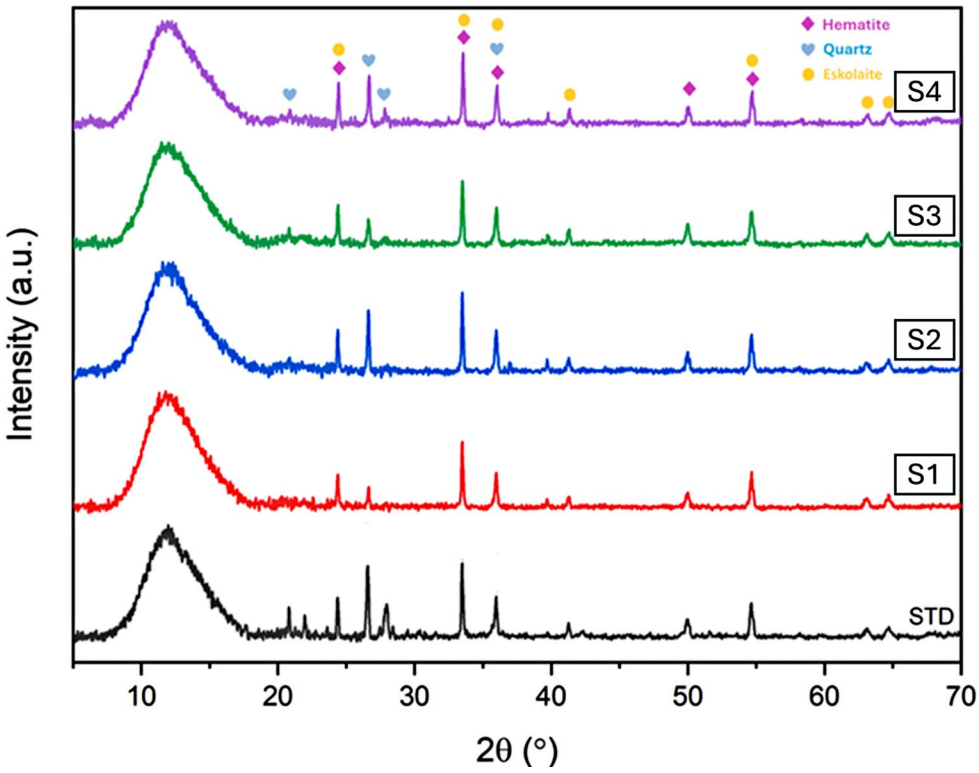


Fig. 5 XRD patterns of the samples

increasing proportions of sludge-derived materials (S1–S4). All diffractograms exhibit a combination of broad amorphous humps, centered approximately at 2θ = 8–17°, associated with the glassy phase, and multiple sharp crystalline reflections. As the sludge content increases from S1 to S4, the intensity of crystalline peaks becomes progressively higher, indicating enhanced crystallinity within the matrix.

Specifically, S4 shows distinct diffraction peaks corresponding to quartz (SiO_2), hematite (Fe_2O_3), and eskolaite (Cr_2O_3) phases, confirming the persistence of crystalline residues originating from the sludge additive. The presence of quartz is expected due to the incomplete melting of silica-rich particles during firing, while hematite and eskolaite can be attributed to the iron and chromium content of the waste material and the intentionally added chromophore agents. Compared to the reference STD sample, which displays relatively lower crystalline peak intensities and a more prominent amorphous halo, the S2–S4 compositions demonstrate an increasingly heterogeneous microstructure with coexisting glassy and crystalline domains.

Overall, these results suggest that the incorporation of higher sludge fractions promotes partial crystallization during thermal treatment, likely as a consequence of the elevated concentrations of refractory oxides (Al_2O_3, Fe_2O_3, Cr_2O_3) and the reduction in alkali fluxes.

Figure 6 shows backscattered electron micrographs of the reference glaze (STD) (a) and the waste-containing formulations (b–e), illustrating the evolution of microstructural features as a function of increasing sludge content. In the STD sample (a), the microstructure is relatively dense and homogeneous, with only isolated bright crystalline inclusions embedded within the glassy matrix. These discrete crystalline phases appear well dispersed and occupy a low area fraction, indicating effective melting and incorporation during firing. In contrast, samples S1 and S2 (b and c) display a higher number density of bright crystalline particles, which are more uniformly distributed across the matrix. The increase in the volume fraction of crystalline inclusions suggests partial crystallization promoted by the introduction of sludge-derived oxides, as supported by the XRD results. In samples S3 and S4 (d and e), the microstructure becomes noticeably more heterogeneous. The population of bright crystalline regions further increases in both size and frequency, indicating significant crystallization processes occurring during cooling. The higher density and partial agglomeration of these crystalline phases reflect the elevated concentrations of refractory components such as Al_2O_3, Fe_2O_3, and Cr_2O_3, coupled with the reduced content of alkali fluxing agents, which collectively limit the complete dissolution of sludge particles into the vitreous phase.

Figure 7 shows the electron micrograph of the standard glaze sample (a) along with the corresponding EDX spectra (b) collected from selected crystalline regions labeled 1–3. The EDX spectrum obtained from region 1 reveals a high concentration of chromium and calcium peaks, with minor contributions of iron and oxygen. This composition suggests

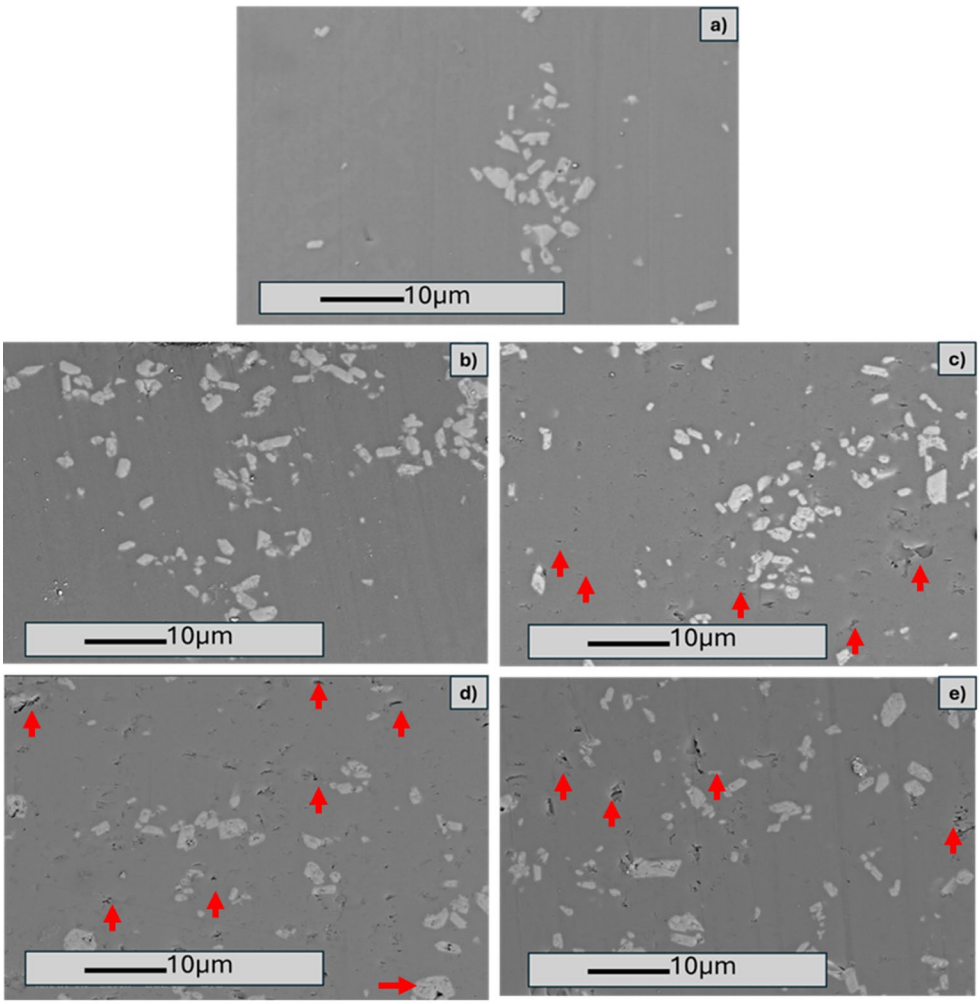


Fig. 6 Backscattered electron microscope images of the samples: (**a**) STD, (**b**) S1, (**c**) S2, (**d**) S3, and (**e**) S4

the presence of chromium-rich crystalline phases, likely corresponding to eskolaite (Cr_2O_3) or a mixed chromium-calcium oxide, which are consistent with the intentionally added chromophore components and the sludge-derived refractory elements. Region 2 exhibits pronounced iron peaks together with calcium and oxygen signals, indicating the presence of iron oxide crystallites such as hematite (Fe_2O_3) or potentially a mixed calcium-iron phase precipitated during cooling. The relative intensity of the iron signal in this area supports the interpretation of localized segregation of iron-rich phases within the matrix. Region 3 shows dominant silicon and oxygen peaks along with detectable aluminum and calcium signals, suggesting the presence of silica-based crystalline domains, most likely residual quartz particles partially incorporated into the glassy matrix. The coexistence of chromium-, iron-, and silica-rich crystalline inclusions, as identified by EDX analysis, correlates well with the XRD results and supports the observation that the glaze microstructure contains crystalline phases embedded in the predominantly amorphous glassy phase.

Figure 8 shows the EDX analysis of the S1 sample. In this figure, the EDX spectrum collected from region 1 indicates the presence of eskolaite crystals, while the spectrum from region 2 reveals hematite crystals, and the spectrum from region 3 demonstrates the presence of quartz signals. The results are consistent with the XRD data. Since the same phases were detected in all samples, only the EDX analysis result of the S1 sample is presented here.

Hardness and mechanical properties of the samples

Figure 5 displays the Vickers hardness values of the reference glaze (STD) and the sludge-containing formulations (S1–S4). The results reveal that the S1 sample achieved the highest hardness value (~ 720 Hv), which can be attributed to its microstructure characterized by a balanced distribution of crystalline phases and relatively low porosity. The presence of uniformly dispersed chromium-rich and iron-rich microcrystals, as confirmed by XRD and EDX analyses, likely acted as effective reinforcement sites within the glassy matrix, enhancing its resistance to localized

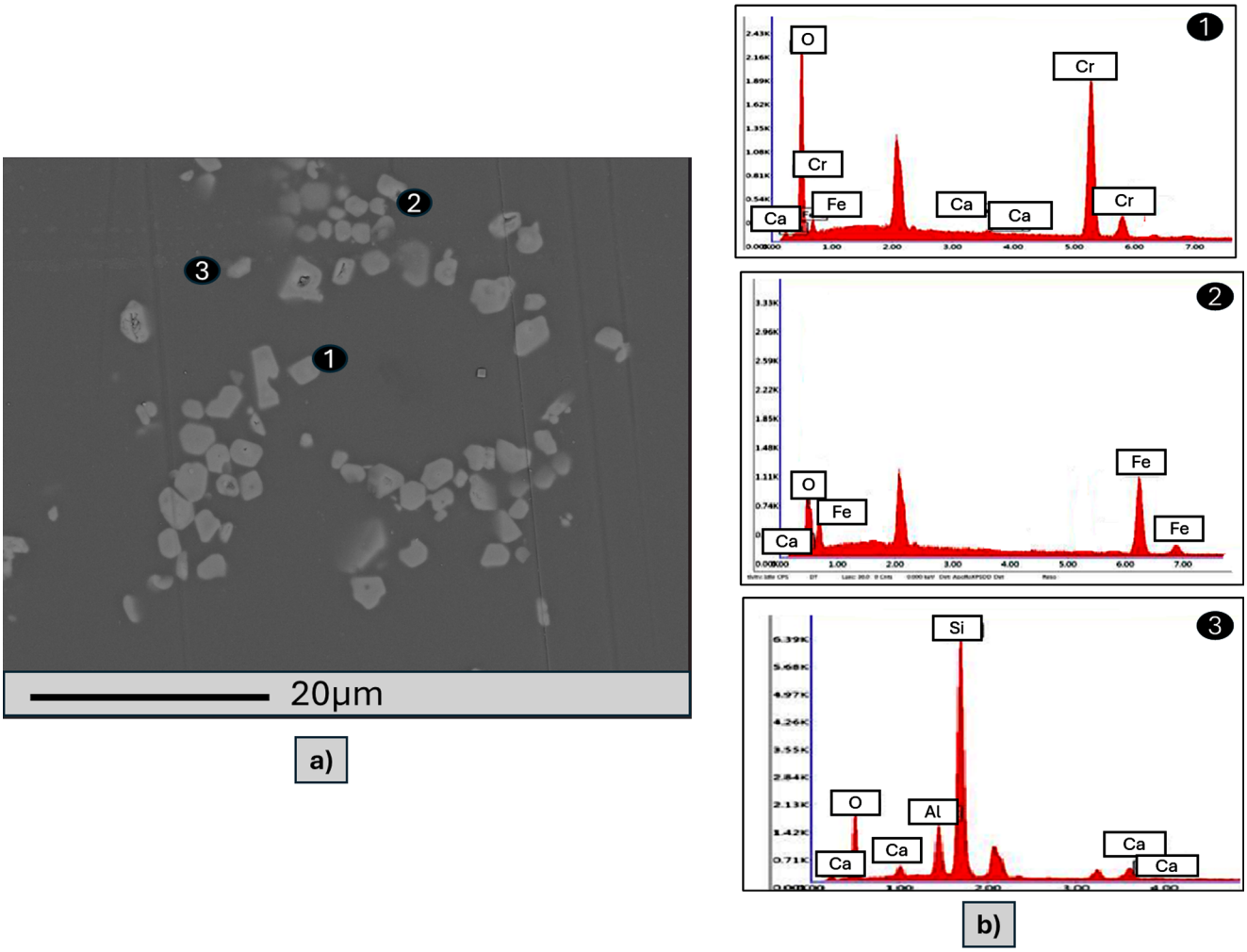


Fig. 7 EDX analysis result of the standard sample (**a**) Microstructure view (**b**) EDX analysis

deformation under indentation [32, 33]. In contrast, the hardness decreased progressively in the S2, S3, and S4 samples. While S2 maintained a moderately high hardness (~ 670 Hv), further increases in sludge content in S3 and S4 led to values comparable to or slightly lower than the reference glaze. This decline in hardness is likely related to the higher degree of microstructural heterogeneity and increased porosity observed in these samples (the areas indicated by arrows in Fig. 6) which may have resulted from incomplete melting of sludge particles and more pronounced crystallization during firing. Such defects can act as stress concentrators, reducing the overall mechanical integrity of the glaze. The reference STD sample exhibited an intermediate hardness (~ 650 Hv), reflecting the contribution of a relatively homogeneous glassy phase with limited crystalline reinforcement (Fig. 9).

The hardness results suggest that a moderate incorporation of sludge (as in S1) can improve hardness due to controlled crystallization and microstructural densification, whereas excessive sludge content adversely affects the mechanical performance due to the development of microstructural discontinuities and increased porosity.

All samples show an overall uniform black surface; however, variations in surface integrity and defect occurrence are evident depending on the amount of sludge incorporated. The STD, S1, and S2 samples display smooth, consistent glaze layers with no major visible flaws. Conversely, S3 and S4 exhibit clear signs of localized surface defects and increased heterogeneity, as marked by the red dashed areas. In particular, S3 shows minor irregularities and incomplete glaze coverage near the perimeter, while S4 contains more severe defects such as clusters of pores and partial detachment of the glaze layer. These visual findings align with the microstructural and compositional results, suggesting that higher sludge levels hinder complete vitrification, elevate melt viscosity during firing, and promote the entrapment of gases or undissolved particles [34–39]. Collectively, these effects compromise surface quality. The results indicate

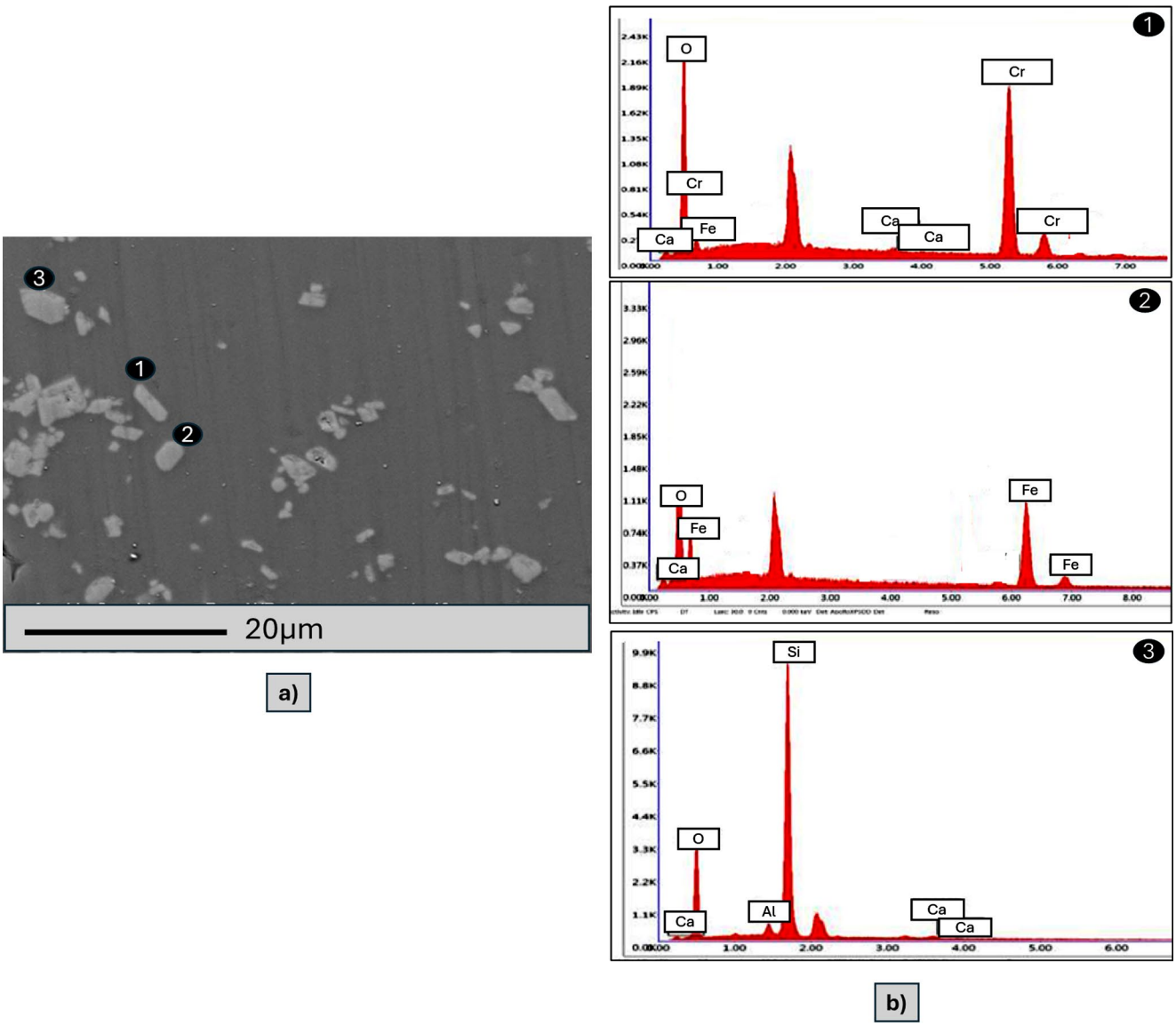


Fig. 8 EDX analysis result of S1 sample (**a**) Microstructure view (**b**) EDX analysis

that moderate sludge substitution retains satisfactory glaze appearance, whereas excessive sludge addition leads to noticeable surface imperfections (Fig. 10).

Conclusions

In this study, İzmit Gulf bottom sludge was successfully utilized as a partial replacement for silica in black opaque wall tile glazes. Rheological measurements revealed that increasing sludge content led to a pronounced rise in viscosity, from 460 mPa·s for the standard glaze to 920 mPa·s for the highest sludge-containing composition (S4). Consistently, thermal analyses showed that the sintering and softening temperatures increased from 734 °C to 798 °C (STD) to 798 °C and 832 °C (S4), indicating enhanced refractory behavior resulting from the sludge's oxide-rich composition. Mechanical characterization demonstrated that microhardness reached a maximum value of approximately 720 Hv in the S1 composition (25 wt% sludge), exceeding both the reference glaze (~650 Hv) and higher sludge-containing samples. The reduction in hardness at elevated sludge levels was attributed to increased porosity and microstructural heterogeneity. Environmental performance was verified through leaching tests, which confirmed that all heavy metal releases remained below regulatory limits. Although chromium leaching increased to 0.03 mg/L in the S4 composition, it remained well below the permissible threshold of 0.05 mg/L, indicating acceptable environmental safety. Overall, the S1 composition emerged as the optimal formulation, offering the most balanced performance by combining

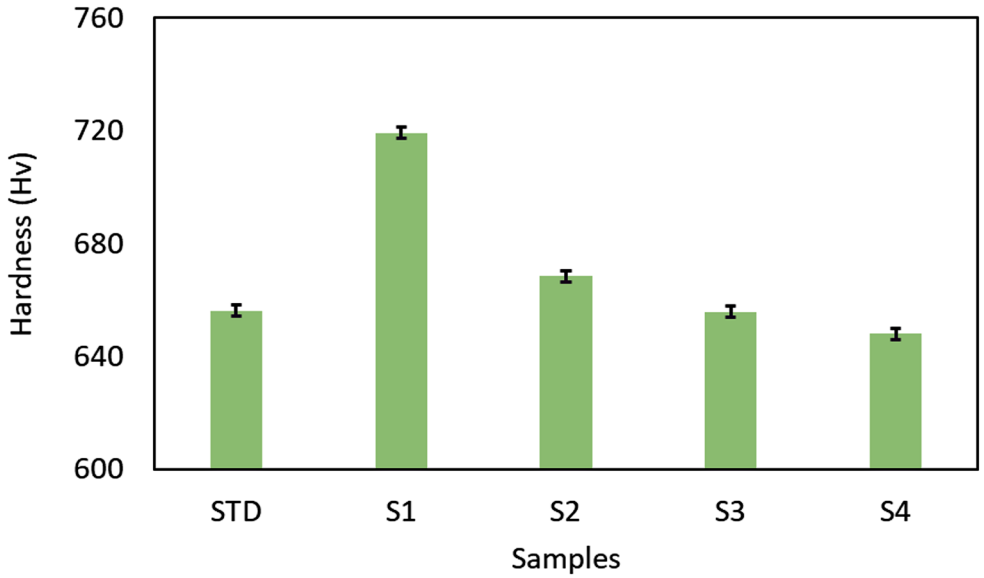


Fig. 9 Hardness test results of the samples



Fig. 10 Post-firing images of the glazed samples after sintering at 1050 °C for 30 min

improved mechanical hardness, acceptable gloss, stable color characteristics, and full compliance with environmental regulations. These results demonstrate that İzmit Gulf bottom sludge can be effectively valorized as a sustainable raw material for black opaque wall tile glazes when used in controlled proportions, supporting resource conservation, waste minimization, and circular economy practices in ceramic production.

Acknowledgements The authors gratefully acknowledge the collaboration and valuable support provided by Kocaeli University in the course of this study.

Author contribution Conceptualization, Dr. Neslihan Tamsü Selli.; Methodology, Dr. Neslihan Tamsü Selli. and Dr. Nermin Demirkol; Investigation, Kübranur Çatalbaş; Writing—Original Draft, Dr. Neslihan Tamsü Selli; Writing—Review & Editing, Dr. Nermin Demirkol; Supervision, Dr. Neslihan Tamsü Selli. All authors have read and agreed to the published version of the manuscript.

Funding Open access funding provided by the Scientific and Technological Research Council of Türkiye (TÜBİTAK).

Data availability The data are available from the corresponding author upon reasonable request.

Declarations

Competing interest The authors declare that they have no known competing financial interest or personal relationship that could have appeared to influence the work reported in this paper.

Open Access This article is licensed under a Creative Commons Attribution 4.0 International License, which permits use, sharing, adaptation, distribution and reproduction in any medium or format, as long as you give appropriate credit to the original author(s) and the source, provide a link to the Creative Commons licence, and indicate if changes were made. The images or other third party material in this article are included in the article's Creative Commons licence, unless indicated otherwise in a credit line to the material. If material is not included in the article's Creative Commons licence and your intended use is not permitted by statutory regulation or exceeds the permitted use, you will need to obtain permission directly from the copyright holder. To view a copy of this licence, visit http://creativecommons.org/licenses/by/4.0/.

References

1. Zanelli, C., Conte, S., Molinari, C., Soldati, R., Dondi, M.: Waste recycling in ceramic tiles: A technological outlook. Resour. Conserv. Recycl. **168**, 105289 (2021)

2. Marín-Cortés, S., Fernández-Álvarez, M., Moure, A., Fernández, J.F., Enríquez, E.: Chemometric-driven quantification of construction and demolition waste using Raman spectroscopy and SWIR: enhancing sustainability in the ceramic sector. Resour. Conserv. Recycl. **199**, 107259 (2023)
3. Arletti, R., Conte, S., Zanelli, C., De Iuliis, M., Di Giuseppe, D., Scognamiglio, V., et al.: Recycling the product of thermal inertization of man-made vitreous fibres for the manufacture of stoneware tiles. Waste Biomass Valor. **14**(5), 1721–1736 (2023)
4. Vantsi, O., K¨arki, T.: Mineral wool waste in europe: A review of mineral wool waste quantity, quality, and current recycling methods. J. Mater. Cycles Waste Manage. 1 Febbraio. **16**, 62–72 (2014)
5. Tamsu Selli, N., Basaran, N.: Valorization of aluminium slags to produce sustainable ceramic wall tiles. J. Aust Ceram. Soc. **59**, 1249–1261 (2023). https://doi.org/10.1007/s41779-023-00905-8
6. Achour, R., Zentar, R., Abriak, N.E., Rivard, P., Gregoire, P.: Durability study of concrete incorporating dredged sediments, case stud. Constr. Mater. **11**, e00244 (2019). https://doi.org/10.1016/j.cscm.2019.e00244
7. Rozière, E., Samara, M., Loukili, A., Damidot, D.: Valorisation of sediments in self-consolidating concrete: mix-design and microstructure. Constr. Build. Mater. **81**, 1–10 (2015). https://doi.org/10.1016/j.conbuildmat.2015.01.080
8. Karius, V., Hamer, K.: pH and grain-size variation in leaching tests with bricks made of harbour sediments compared to commercial bricks. Sci. Total Environ. **278**, 73–85 (2001). https://doi.org/10.1016/S0048-9697(00)00889-5
9. Samara, M., Lafhaj, Z., Chapiseau, C.: Valorization of stabilized river sediments in fired clay bricks: Factory scale experiment. J. Hazard. Mater. **163**, 701–710 (2009). https://doi.org/10.1016/j.jhazmat.2008.07.153
10. Amar, M., Benzerzour, M., Safhi, A.E.M., Abriak, N.E.: Durability of a cementitious matrix based on treated sediments, case stud. Constr. Mater. **8**, 258–276 (2018). https://doi.org/10.1016/j.cscm.2018.01.007
11. Dang, T.A., Kamali-Bernard, S., Prince, W.A.: Design of new blended cement based on marine dredged sediment. Constr. Build. Mater. **41**, 602–611 (2013). https://doi.org/10.1016/j.conbuildmat.2012.11.088
12. Said, I., Missaoui, A., Lafhaj, Z.: Reuse of Tunisian marine sediments in paving blocks: Factory scale experiment. J. Clean. Prod. **102**, 66–77 (2015). https://doi.org/10.1016/j.jclepro.2015.04.138
13. Missaoui, A., Said, I., Lafhaj, Z., Daoued, S., Ali, I.B.H.: Laboratory study on recycling of sediments in paving blocks. Environ. Geotech. **3**, 397–407 (2016). https://doi.org/10.1680/envgeo.15.00006
14. Aoual-Benslafa, F.K., Kerdal, D., Ameur, M., Mekerta, B., Semcha, A.: Durability of mortars made with dredged sediments. Procedia Eng. **118**, 240–250 (2015). https://doi.org/10.1016/j.proeng.2015.08.423
15. Laoufi, L., Senhadji, Y., Benazzouk, A.: Valorization of mud from fergoug dam in manufacturing mortars, case stud. Constr. Mater. **5**, 26–38 (2016). https://doi.org/10.1016/j.cscm.2016.06.002
16. Miraoui, M., Zentar, R., Abriak, N.E.: Road material basis in dredged sediment and basic oxygen furnace steel slag. Constr. Build. Mater. **30**, 309–319 (2012). https://doi.org/10.1016/j.conbuildmat.2011.11.032
17. Siham, K., Fabrice, B., Edine, A.N., Patrick, D.: Marine dredged sediments as new materials resource for road construction. Waste Manag. **28**, 919–928 (2008). https://doi.org/10.1016/j.wasman.2007.03.027
18. Loudini, A., Ibnoussina, M., Witam, O., Limam, A., Turchanina, O.: Valorisation of dredged marine sediments for use as road material. Case Stud. Constr. Mater. **13** (2020). ISSN 2214–5095. https://doi.org/10.1016/j.cscm.2020.e00455
19. Tamsu Selli, N., Basaran, N.: Controlling the hardness and wear resistance of opaque white glaze by addition of halloysite clay in the composition. Bol. Soc. Esp. Ceram. Vidrio **62**(3), 243–256 (2023). https://doi.org/10.1016/j.bsecv.2022.01.002
20. Sisti, M., Guidetti, D., Altimari, F., Andreola, F., Barbieri, L., Lancellotti, I., Casini, L., Colombo, F., Arletti, R., Fantini, R., Gualtieri, A.F.: Sustainable glazes for ceramic tiles: exploiting inertized man-made vitreous fibres waste as a resource. Ceram. Int. **51**(4), 4195–4205 (2025). https://doi.org/10.1016/j.ceramint.2024.11.396
21. Dana, K., Sinhamahapatra, S., Tripathi, H.S., Ghosh, A.: Refractories of Alumina-Silica system. Trans. Indian Ceram. Soc. **73**(1), 1–13 (2014). https://doi.org/10.1080/0371750X.2014.905265
22. Pagona, E., Kalaitzidou, K., Zaspalis, V., Zouboulis, A., Mitrakas, M.: Effects of MgO and Fe_2O_3 addition for upgrading the refractory characteristics of magnesite ore mining Waste/By-Products. Clean. Technol. **4**, 1103–1126 (2022). https://doi.org/10.3390/cleantechnol4040067
23. Karlsson, S.: Viscosity of alumina doped soda lime silicate glasses – observation of anomaly in the linear increase as Al_2O_3 replaces SiO_2. J. Non-cryst. Solids. **573**, 121149 (2021). https://doi.org/10.1016/j.jnoncrysol.2021.121149 ISSN 0022-3093
24. Cheng, J., Xiao, Z., Yang, K., Wu, H.: Viscosity, fragility and structure of Na_2O–CaO–Al_2O_3–SiO_2 glasses of increasing Al/Si ratio, ceramics international, **39**(4), 4055–4062, ISSN 0272–8842 (2013). https://doi.org/10.1016/j.ceramint.2012.10.258
25. Di Genova, D., Vasseur, J., Hess, K.-U., Neuville, D.R., Dingwell, D.B.: Effect of oxygen fugacity on the glass transition, viscosity and structure of silica- and iron-rich magmatic melts. J. Non-cryst. Solids. **470**, 78–85 (2017). ISSN 0022-3093 https://doi.org/10.1016/j.jnoncrysol.2017.05.003
26. Liu, W., Zuo, H.: Mixed influence of Na_2O and K_2O on the viscous properties of aluminosilicate melt. Ceram. Int. **51**, 17131–17137, ISSN 0272–8842 (2025). https://doi.org/10.1016/j.ceramint.2025.01.487
27. Dong, W., Bao, Q., Zhou, J., Zhao, T., Liu, K., Hu, Z.: Preparation of porcelain Building tiles using K_2O–Na_2O feldspar flux as a modifier agent of low-temperature firing. J. Ceram. Soc. Jpn. **125**(9), 690–694 (2017). ISSN 1882 – 0743 https://doi.org/10.2109/jcersj2.163270
28. Li, C.-T., Lee, W.-J., Huang, K.-L., Fu, S.-F., Lai, Y.-C.: Vitrification of chromium electroplating sludge. Environ. Sci. Technol. **41**(9), 2950–2956 (2007). https://doi.org/10.1021/es062273b ISSN 0013–936X
29. Chou, I.-C., Wang, Y.-F., Chang, C.-P., Wang, C.-T., Kuo, Y.-M.: Effect of NaOH on the vitrification process of waste Ni–Cr sludge. J. Hazard. Mater. **185**, 2–3 (2011). https://doi.org/10.1016/j.jhazmat.2010.10.089
30. Rezvani, M., Eftekhari-Yekta, B., Solati-Hashjin, M., Marghussian, V.K.: Effect of Cr_2O_3, Fe_2O_3 and TiO_2 nucleants on the crystallization behaviour of SiO_2–Al_2O_3–CaO–MgO(R_2O) glass-ceramics. Ceram. Int. **31**(1), 75–80 (2005). https://doi.org/10.1016/j.ceramint.2004.06.001
31. Hrma, P., Vienna, J.D., Wilson, B.K., Plaisted, T.J., Heald, S.M.: Chromium phase behavior in a multi-component borosilicate glass melt. J. Non-cryst. Solids. **352**, 21–22 (2006). https://doi.org/10.1016/j.jnoncrysol.2006.02.073
32. Ercenk, E., Basaran, T., Yilmaz, S.: The effect of chromite ore addition on crystallization kinetics of basalt based machinable glass-ceramics. Ceram. Int. **47**(12), 16902–16917 (2021). https://doi.org/10.1016/j.ceramint.2021.02.098
33. Pekkan, K., Gün, Y.: Effect of different metal oxides on Vickers hardness of the frit based crystalline glazes. Nevşehir Bilim ve Teknoloji Derg. **7**(1), 32–40 (2018). https://doi.org/10.17100/nevbiltek.368987

34. Tan, S., Chang, J., Liu, X., Sun, S., Xian, L., Zhang, S.: Influence of radioactive sludge content on vitrification of high-level liquid waste. Sustainability **15**(6), 4937 (2023). https://doi.org/10.3390/su15064937
35. Varitis, S., Kavouras, P., Pavlidou, E., Pantazopoulou, E., Vourlias, G., Chrissafis, K., Zouboulis, A.I.: Th. Karakostas, and Ph. Komninou, vitrification of incinerated tannery sludge in silicate matrices for chromium stabilization. Waste Manage. **59**, 237–246 (2017). https://doi.org/10.1016/j.wasman.2016.10.012
36. Rennie, M.S., Howat, D.D., Jochens, P.R.: The effects of chromium oxide, iron oxide and calcium oxide on the Liquidus temperatures, viscosities and electrical conductivities of slags in the system $MgO–Al_2O_3–SiO_2$. J. South. Afr. Inst. Min. Metall. **73**(1), 1–9 (Aug. 1972)
37. Babenko, A.A., Zaitsev, A.V., Bratchuk, A.M.: Effect of basicity and chromium oxide on the viscosity of boron-containing slags. IOP Conf. Ser.: Mater. Sci. Eng. **966**, 012012 (2020). https://doi.org/10.1088/1757-899X/966/1/012012
38. Zhao, M., Cao, J., Geng, X., Song, W., Wang, Z.: Structural origin of $CaO–MgO–Al_2O_3–SiO_2–Fe_2O_3$ glass crystallization: iron-containing clusters. J. Non-Cryst. Solids **547**, 120295 (2020). https://doi.org/10.1016/j.jnoncrysol.2020.120295
39. Pokorny, R., Hrma, P.: Model for the conversion of nuclear waste melter feed to glass. J. Nucl. Mater. **445**, 190–199 (2014). https://doi.org/10.1016/j.jnucmat.2013.10.051

Publisher's note Springer Nature remains neutral with regard to jurisdictional claims in published maps and institutional affiliations.